Chemistry–A European Journal
Research Article
doi.org/10.1002/chem.202303798
Chemistry Europe
European Chemical Societies Publishing
www.chemeurj.org

Circularly Polarized Luminescence of Thiophene-Bridged Macrocyclic pseudo-*meta* [2.2]Paracyclophanes

Charlotte Kress[+],[a] Eric Sidler[+],[a] Payton Downey,[d] Patrick Zwick,[a] Olaf Fuhr,[b, c] Dieter Fenske,[b] Stefan Bernhard,[d] and Marcel Mayor*[a, b, e]

Chiral organic molecules possessing high quantum yields, circular dichroism, and circularly polarized luminescence values have great potential as optically active materials for future applications. Recently, the identification of a promising class of inherently chiral compounds was reported, namely macrocyclic 1,3-butadiyne-linked pseudo-*meta*[2.2]paracyclophanes, displaying high circular dichroism and related g_{abs} values albeit modest quantum yields. Increasing the quantum yields in an attempt to get bright circularly polarized light emitters, the high-yielding heterocyclization of those 1,3-butadiyne bridges resulting in macrocyclic 2,5-thienyls-linked pseudo-*meta* [2.2]paracyclophanes is herein described. The chiroptical properties of both, the previously reported 1,3-butadiyne, and the novel 2,5-thienyl bridged macrocycles of various sizes, are experimentally recorded, and theoretically described using density-functional theory.

Introduction

Since the discovery of [2.2]paracyclophane (PCP) by Brown and Farthing in 1949,[1] this unique building block has found its way in numerous research fields including optoelectronics, molecular electronics and conjugated polymers.[2] PCPs are highly strained cyclophanes where two phenylenes are bridged by two ethylene linkers. The face-to-face oriented benzene units are slightly rotated with respect to each other and their planar distance of about 3.1 Å results in strong π–π interaction.[3,4] The functionalization of PCPs was a breakthrough and allowed their introduction in more complex molecular architectures resulting in various novel 3D materials.[2] Especially the four pseudo disubstitution patterns[5] have caught the attention of molecular engineers due to their different geometries and in some cases even inherent chirality. Three of the pseudo-substituted PCP units, namely pseudo-*ortho*,[6,7] pseudo-*meta*[8,9] and pseudo-*para*,[10] were recently embedded in macrocyclic structures, equipping the respective molecules with exemplary chiroptics – a highly sought after property in optoelectronic materials. Besides different geometries, the PCP substitution patterns also display substantial differences in the electronic structure and electronic coupling through the 3D building block. For pseudo-*meta* PCPs constructive quantum interference was hypothesized theoretically[11] and corroborated experimentally,[4] suggesting the building block to be a valuable subunit for conjugated materials. This led us to our recent work of thoroughly conjugated macrocycles incorporating several pseudo-*meta* PCPs interlinked by 1,3-butadiyne units.[8] The reported library $(R_p)_n$-**2$_n$**, where n represents the number of PCP subunits (Figure 1a), displayed unprecedented circular dichroism (CD) intensities and was synthetically accessible in high yields thanks to the predefined angle of the pseudo-*meta* PCP subunit. The large absorption dissymmetry factors g_{abs} (where $g_{abs}=\Delta\varepsilon/\varepsilon$) of 0.021 for $(R_p)_4$-**2$_4$** now urged the investigation of their circularly polarized luminescence (CPL) properties, particularly given the recently reported correlation of $|g_{lum}|=0.94\times|g_{abs}|$ for planar chiral cyclophanes[12] (where $g_{lum}=2(I_L-I_R)/(I_L+I_R)$ and I is the CPL intensity). Simultaneously, we aimed at improving the molecular structure to enhance photostability, quantum yield and chiroptical properties to render them more desirable towards future applications.[13] In recent literature reports, the transformation of 1,3-butadiynes to 2,5-thienyls has led to a concurrent increase of quantum yield and photostability given the reduced number of photoreactive alkynes.[14,15,16] Herein, we thus show the synthesis and characterization of the heterocyclized library $(R_p)_n$-**1$_n$**, and investigate and compare the

[a] C. Kress,[+] Dr. E. Sidler,[+] Dr. P. Zwick, Prof. Dr. M. Mayor
Department of Chemistry
University of Basel
St. Johanns-Ring 19, 4056 Basel, Switzerland
E-mail: marcel.mayor@unibas.ch
[b] Dr. O. Fuhr, Prof. Dr. D. Fenske, Prof. Dr. M. Mayor
Institute for Nanotechnology (INT)
Karlsruhe Institute of Technology (KIT)
P. O. Box 3640, 76021 Karlsruhe, Germany
[c] Dr. O. Fuhr
Karlsruhe Nano Micro Facility (KNMFi)
Karlsruhe Institute of Technology (KIT)
Kaiserstraße 12, 76131 Karlsruhe, Germany
[d] P. Downey, Prof. Dr. S. Bernhard
Department of Chemistry
Carnegie Mellon University
15213 Pittsburgh, Pennsylvania, USA
[e] Prof. Dr. M. Mayor
Lehn Institute of Functional Materials (LIFM)
School of Chemistry
Sun Yat-Sen University (SYSU)
510275 Guangzhou, China
[+] Equal contributing first authors.

Supporting information for this article is available on the WWW under https://doi.org/10.1002/chem.202303798

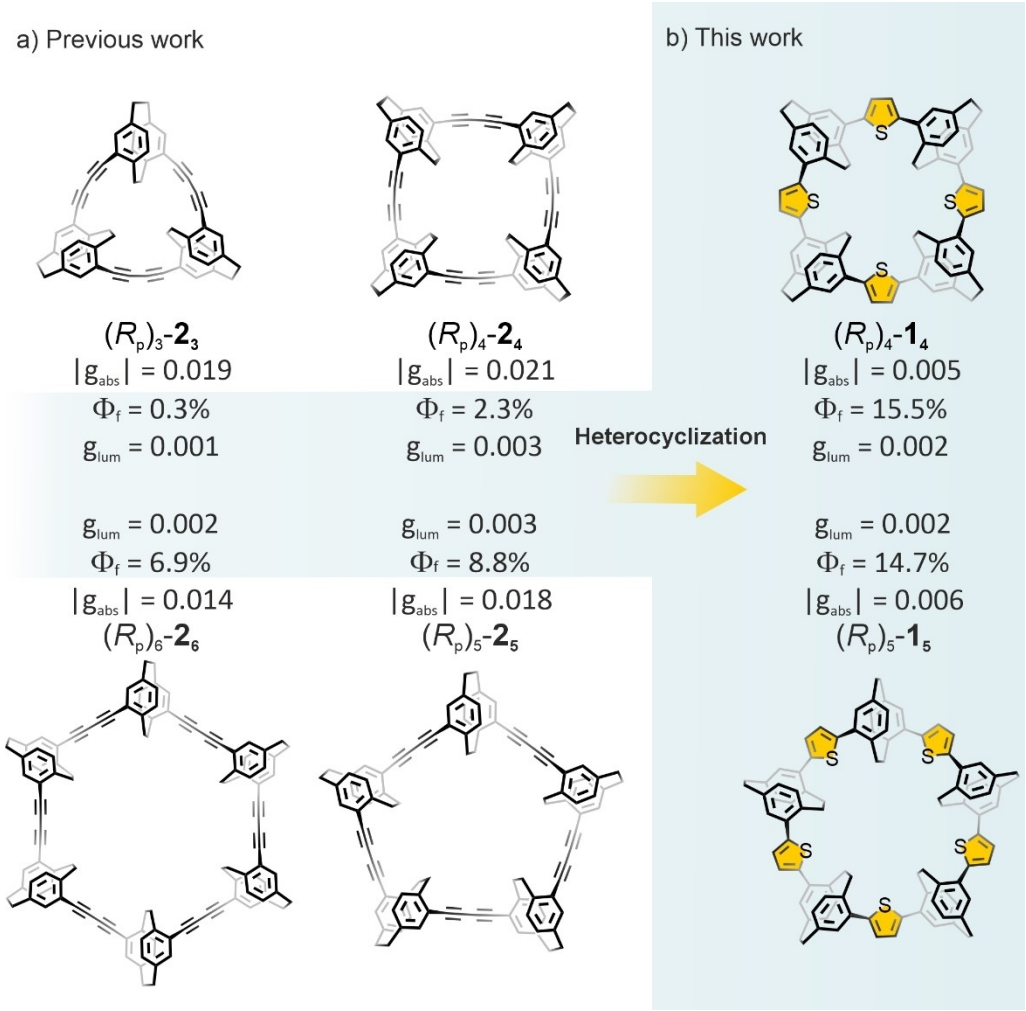

Figure 1. Comparison of our previous (a) and current work (a and b, underlined by blue colored background) highlighting the main (chir)optical properties of the molecules.

promising CPL properties of both libraries $(R_p)_n$**1**$_n$ and $(R_p)_n$**2**$_n$ (Figure 1b). We thereby set our focus on the trimeric, tetrameric and pentameric macrocycles $(R_p)_3$-**2**$_3$, $(R_p)_4$-**2**$_4$, and $(R_p)_5$-**2**$_5$. The library of thienyl-linked macrocycles $(R_p)_n$-**1**$_n$ was not extended to the hexameric structure, as our previous study already showed a significant drop in Cotton effect intensity in the CD experiment. The enantiopure synthesis of the 1,3-butadiyne-linked macrocycles allowed us to work in an enantiopure fashion, not requiring additional chiral separation techniques. Both the synthesis and spectroscopic analysis were performed for each enantiomer, but for simplicity reasons the discussion of the synthesis and optical properties will be limited to the (R_p)-enantiomer.

Results and Discussion

Synthesis and Characterization

We envisioned to introduce the sulfur heteroatom via literature-known heterocyclization procedures starting from the 1,3-butadiyne derivatives $(R_p)_n$-**2**$_n$. The trimeric macrocycle $(R_p)_3$-**2**$_3$ was the first structure that was subjected to the heterocyclization reaction (Scheme 1a). Unfortunately, employing standard literature conditions,[16–19] no product could be isolated and also no corresponding mass signal was observed using matrix-assisted laser desorption/ionization mass spectrometry (MALDI-MS). However, we observed full consumption of the starting compound and conversion to a baseline spot on the thin-layer chromatography (TLC) experiment. Attempts at optimizing the reaction outcome by varying the employed conditions were unsuccessful (see Table S1 in Supporting Information). Since the formation of a 2,5-thienyl generally leads to a contraction in comparison to the 1,3-butadiyne unit, we hypothesized that the trimeric macrocycle is of a too narrow dimension, leading to steric clashes of the ethylene bridges in the center of the ring structure. We assume that the sulfide ion does undergo addition to the 1,3-butadiyne but does not convert to the thiophene unit, which would explain the formation of a polar baseline spot on the TLC. Our efforts to form the thiophene moieties by increasing the temperature (up to 140 °C) were, however, unsuccessful.

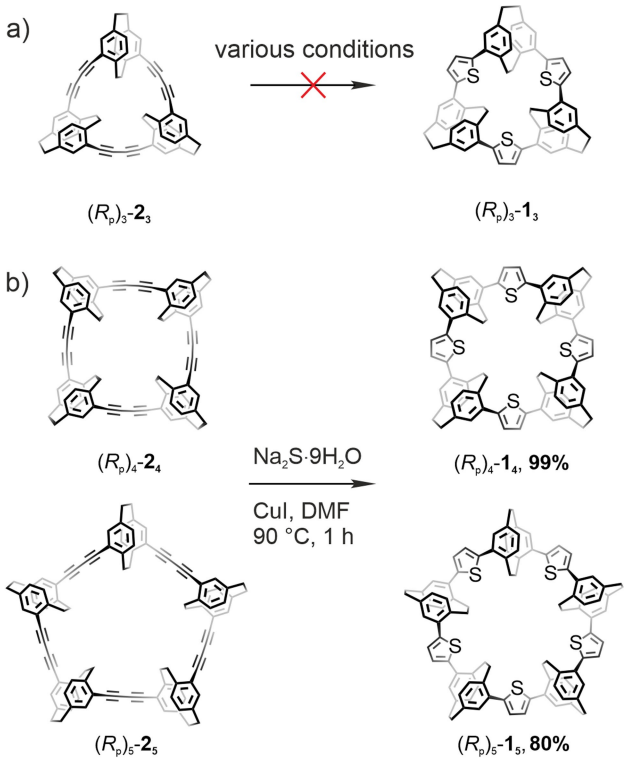

Scheme 1. Synthesis towards $(R_p)_3$-**1**$_3$, $(R_p)_4$-**1**$_4$, and $(R_p)_5$-**1**$_5$. The synthesis of the other enantiomers is not depicted here and can be found in the Supporting Information.

The outcome of the heterocyclization reaction on the tetrameric structure $(R_p)_4$-**2**$_4$ was much more satisfactory. After a few optimization steps, $(R_p)_4$-**1**$_4$ was accessible in 99%, when using sodium sulfide nonahydrate and catalytic amounts of copper iodide in DMF at 90 °C (Scheme 1b). $(R_p)_5$-**2**$_5$ underwent heterocyclization under the same conditions to yield $(R_p)_5$-**1**$_5$ in 80%. The other enantiomers $(S_p)_4$-**1**$_4$ and $(S_p)_5$-**1**$_5$ were synthesized in similar yields of 92% and 77% starting from $(S_p)_4$-**2**$_4$ and $(S_p)_5$-**2**$_5$, respectively, demonstrating the reproducibility of the synthetic protocol.

The successfully synthesized structures $(R_p)_4$-**1**$_4$ and $(R_p)_5$-**1**$_5$ were fully characterized by high-resolution-(HR)-MS analysis and state of the art two-dimensional nuclear magnetic resonance (NMR) spectroscopy, allowing assignment of all signals. In the ^{1}H-NMR spectra shown in Figure 2, the formation of the thiophene can be readily identified by the emergence of a singlet in the aromatic region, which is downfield shifted by 0.11 ppm for $(R_p)_5$-**1**$_5$ compared to $(R_p)_4$-**1**$_4$. This difference in chemical shift can be attributed to a deshielding of the thiophene proton by the ring current of the adjacent PCP-phenylene, which is more pronounced in the pentameric structure due to a smaller ring strain and thus shorter inter-ring distance. The same reasoning could potentially be applied to proton 1, which, however, shows the complete opposite behavior with an upfield shift of 0.13 ppm for $(R_p)_5$-**1**$_5$ compared to $(R_p)_4$-**1**$_4$. In this case, the effect of the strain-release on the PCP core and thus on the face-to-face stacking possibly counteracts the effect of the vicinity of the adjacent π-system. Similarly, the macrocyclic ring strain likely explains the upfield shift of 0.13 ppm for proton 3 in $(R_p)_4$-**1**$_4$ compared to $(R_p)_4$-**1**$_5$. In the tetrameric structure, proton 3 tends to hover on top of the thiophene moiety, leading to a shielding by the diatropic ring current of the thiophene unit. The mentioned effects have only a minor influence on the chemical shift of proton 2, explained by the larger distance to the thiophene ring.

Similar to the 1,3-butadiyne-linked library $(R_p)_n$-**2**$_n$, the ethylene bridge protons in $(R_p)_n$-**1**$_n$ have split up to four individual multiplet signals, which show significant chemical shift differences as compared to terminal acetylene (R_p)-**S1**. The downfield shift of inner proton H_a of $(R_p)_n$-**1**$_n$ can be attributed to the spatial vicinity to the aromatic thiophene moiety and its ring current. This effect is less pronounced for inner proton H_b, which possesses a larger distance to the thiophene unit. Comparable to the 1,3-butadiyne-linked macrocycles $(R_p)_n$**2**$_n$, the chemical shift differences of the outer protons H_a and H_b are less striking due to the larger distance to the linker unit. Generally, the ethylene bridge protons tend to shift towards the signals of the free acetylene starting material (R_p)-**S1** upon enlarging the ring size, nicely reflecting the release of strain. Overall, the ^{1}H-NMR spectrum does not indicate any global aromaticity or antiaromaticity around the macrocyclic circumference.

The structure of $(S_p)_4$-**1**$_4$ was corroborated by x-ray crystallography. Single crystals were obtained by diffusion of isopropanol vapors into a solution of $(S_p)_4$-**1**$_4$ in toluene. The adopted shape of the molecule in the solid state resembles a square with near identical distances of 5.36 to 5.39 Å between the pseudo-*meta* carbons of adjacent PCPs (Figure 3). This is considerably shorter (1.1–1.3 Å) than the distance in the solid-state of the previously reported 1,3-butadiyne-linked tetramer $(S_p)_4$-**2**$_4$, reflecting the aforementioned contraction upon heterocyclization. It is noticeable that the pseudo-*meta* substitution position of the PCP shows a larger angle towards the inside of the macrocyclic structure (122°–124°) compared to the outside (117°–119°). This was unexpected for a square shape and indicates that the thiophenes span an arch, resulting in an overall rather cyclic structure. The sulfur atoms of all thiophenes are pointing towards the inside of the macrocycle and the inner angle was measured to be between 93° and 95°. The angle is sharper than what we would expect for a regular pentagon (108°). From all three single molecule views it is possible to see that the thiophenes adopt different rotational positions in respect to the PCPs, resulting in significantly different torsion angles ranging from 20° to 58°. This indicates rotational flexibility of the thiophenes in the macrocyclic structure, most likely hindering efficient overall conjugation.[20] Regarding the 3D structure, a steepness of 22.6° between the PCP units can be measured, which is larger than for the 1,3-butadiyne-linked tetramer $(R_p)_4$-**2**$_4$, being coherent with the smaller overall ring size.

The unit cell of the crystal structure contains 4 enantiopure molecules, which are displaced laterally and in depth. From the top view as well as from the unit cell, it is possible to see that a PCP unit is placed on top of the cavity of a neighboring macrocycle, such that two thiophenes are oriented face-to-face

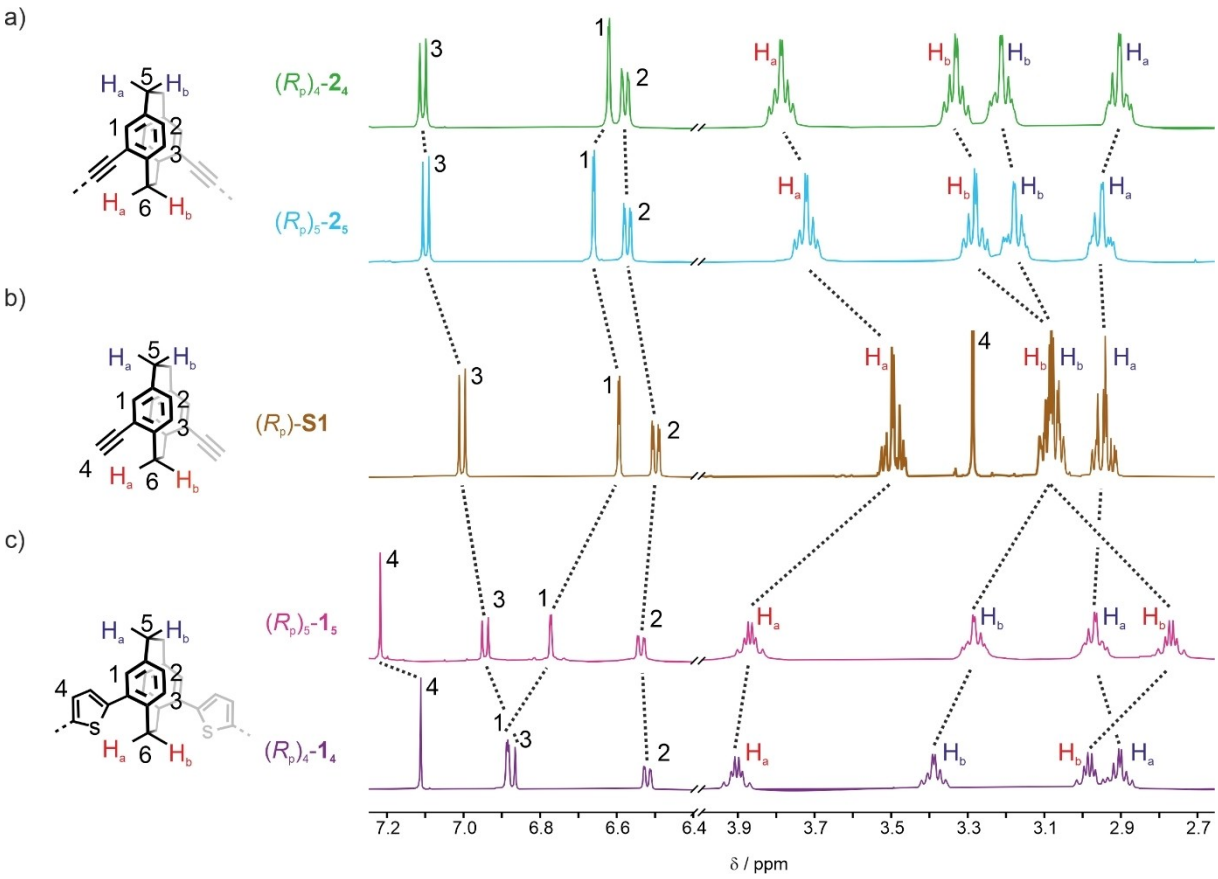

Figure 2. ^{1}H-NMR spectra (500 MHz, $CDCl_3$, 298 K) comparison of starting materials $(R_p)_4$-**2**$_4$ and $(R_p)_5$-**2**$_5$ (a), free acetylene macrocyclization precursor (R_p)-**S1** (b) and thiophene-linked $(R_p)_4$-**1**$_4$ and $(R_p)_5$-**1**$_5$ (c).

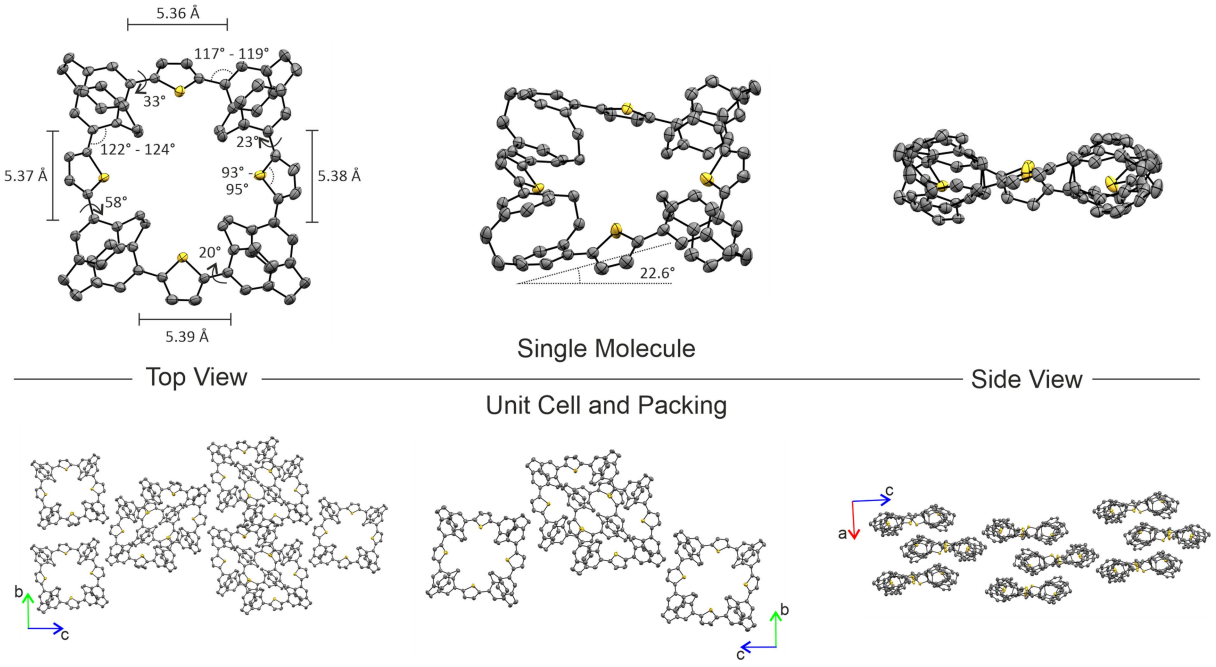

Figure 3. Oak Ridge Thermal Ellipsoid Plots (ORTEP) of the solid-state structure of $(S_p)_4$-**1**$_4$. Single molecules as well as the packing is shown from different sides, while hydrogen atoms, the second position of a sulfur atom and solvent molecules (toluene) are omitted for clarity. The thermal ellipsoids are plotted on a 50% probability.

to each other. The packing does not allow to fill the cavity of $(S_p)_4$-**1₄** (diameter of about 7 Å) with solvent molecules. While no intermolecular π–π stacking is observed, the rather short distance (< 3 Å) of the outer ethylene bridge protons to the neighboring PCP phenylene indicates a favorable CH–π interaction. From the side view, the lateral displacement and spatially tight and interlocked packing gets apparent.

Optical properties

The (chir)optical data of tetrameric and pentameric structures $(R_p)_4$-**1₄**, $(R_p)_5$-**1₅**, $(R_p)_4$-**2₄** and $(R_p)_5$-**2₅** are plotted in Figure 4 and the main values are summarized in Table 1. The absorption spectra of $(R_p)_4$-**1₄** and $(R_p)_5$-**1₅** show one main broad peak with a significant drop in extinction coefficient by a factor of 2.4 and 2.1, as compared to the 1,3-butadiyne-linked macrocycles $(R_p)_4$-**2₄** and $(R_p)_5$**2₅**, respectively. The absorption of $(R_p)_4$-**1₄** and $(R_p)_5$-**1₅** furthermore extends into a redshifted region up to 415 nm. This bathochromic shift could be indicative of an increase in conjugation. Considering the flexibility of the thiophenes already in the solid-state, however, we assume the shift arises due to the electron-donating and HOMO-stabilization effect of the thiophenes.[14][16] This is consistent with the observation of an additional redshift of the absorption maximum when going from the tetrameric $(R_p)_4$-**1₄** (331 nm) to pentameric $(R_p)_5$-**1₅** (340 nm) macrocycle. Such shifts within the same series of compounds were not detected for the $(R_p)_n$-**2ₙ** library. The poor vibronic fine structure resolution of the absorption transitions in $(R_p)_n$-**1ₙ** possibly also arises from the increased number of degrees of freedom of the thiophenes compared to the 1,3-butadyines, similar to previous reports.[14,20]

The emission spectra of the thiophene derivatives are significantly red shifted compared to the 1,3-butadiyne ones resulting in a larger *Stokes* shift, being consistent with a higher flexibility. For $(R_p)_4$-**1₄** and $(R_p)_5$-**1₅** one main broad emission peak at 452 nm and 439 nm, respectively, can be observed, while for both species a blue shifted shoulder arises (430 nm and 425 nm). The shape and low vibronic resolution of the spectra are in good agreement with the discussed absorption spectra. The presence of a shoulder in the emission spectrum, however, possibly indicates a more rigid structure in the excited state than in the ground state. The quantum yields (Φ_f) for $(R_p)_4$-**1₄** and $(R_p)_5$-**1₅** were determined to be 15.5% and 14.7%, respectively, while the values for the $(R_p)_n$-**2ₙ** library are below 10% for all the compounds (Table 1). Overall, the values match literature results and meet our primary goal to increase the quantum yield of pseudo-*meta*-PCP macrocyclic structures with the intention to move the application potential of such structure into the focus of interest.

The CD spectra of $(R_p)_4$-**1₄** and $(R_p)_5$-**1₅** show three main *Cotton* bands at similar wavelengths (Figure 4b). The enantiomers show the same response with opposite sign, resulting in mirrored traces, indicative of absence in racemization during the reaction conditions. The signal intensity of the thiophenes is rather weak, reaching maximal values of $-119\ L\,mol^{-1}\,cm^{-1}$ (361 nm) for $(R_p)_4$-**1₄** and $-195\ L\,mol^{-1}\,cm^{-1}$ (368 nm) for $(R_p)_5$**1₅**. Both species have two additional main *Cotton* bands with lower intensities and opposite signs as reported in Table 1. The CD response of $(R_p)_5$-**1₅** is slightly stronger compared to $(R_p)_4$-**1₄**, consistent with the increased extinction coefficient of $(R_p)_5$-**1₅** in the absorption spectrum. The *Cotton* effect intensities of the thiophene derivatives are with a factor of seven significantly lower than the one of the $(R_p)_n$-**2ₙ** library. Given that the decrease in molar CD is much larger than in the absorption spectrum, the g_{abs} values dropped to ~5×10^{-3} for both compounds in the $(R_p)_n$-**1ₙ** library. This possibly indicates a smaller contribution of the magnetic transition dipole moment for $(R_p)_n$-**1ₙ** or an unfavorable orientation of the magnetic in relation to the electric transition dipole moment in the ground state.[21] Also, there is literature precedence of flexible molecules showcasing decreased chiroptical properties, all being consistent with our observations.[22,23]

The CPL of the tetrameric and pentameric macrocyclic structures is depicted in Figure 4d. The excess emission of circularly polarized light accounted for 0.13% and 0.14% of the total emission for $(R_p)_4$-**2₄** and $(R_p)_5$-**2₅** respectively. To quantify the amount of chiral light emission, g_{lum} values were calculated

Table 1. Comparison of the optical properties of the discussed derivatives $(R_p)_4$-**1₄**, $(R_p)_5$-**1₅**, $(R_p)_3$-**2₃**, $(R_p)_4$-**2₄**, $(R_p)_5$-**2₅** and $(R_p)_6$-**2₆**.

Comp.	$\varepsilon_{\lambda max}$ (λ_{max}) [L mol^{-1} cm^{-1}]	λ_{em} (excitation) [nm]	Φ_f (excitation)	$\Delta\varepsilon_\lambda$ (λ) [L mol^{-1} cm^{-1}]			g_{abs} (λ)	$\Delta I/I$	g_{lum}
$(R_p)_4$-**1₄**	44263 (331 nm)	430, 452 (335)	15.5% (335 nm)	−119 (361 nm)	56 (303 nm)	67 (240 nm)	−0.0051 (381 nm)	0.08%	0.002
$(R_p)_5$-**1₅**	62824 (340 nm)	425, 439 (335)	14.7% (335 nm)	−195 (368 mn)	64 (300 nm)	67 (240 nm)	−0.0058 (383 nm)	0.04%	0.002
$(R_p)_3$-**2₃**	45911 (369 nm)[a]	385, 410 (330)[a]	0.3% (335 nm)	−523 (376 nm)[a]	−220 (348 nm)	−531 (231 nm)	−0.019 (379 nm)	0.05%	0.001
$(R_p)_4$-**2₄**	106275 (370 nm)[a]	385, 410 (340)[a]	2.3% (335 nm)	−1168 (377 nm)[a]	−344 (349 nm)	−568 (229 nm)	−0.021 (380 nm)	0.13%	0.003
$(R_p)_5$-**2₅**	134695 (370 nm)[a]	385, 410 (340)[a]	8.8% (335 nm)	−1247 (376 nm)[a]	−353 (349 nm)	−586 (230 nm)	−0.018 (380 nm)	0.14%	0.003
$(R_p)_6$-**2₆**	137382 (370 nm)[a]	385, 410 (340)[a]	6.9% (335 nm)	−1049 (375 nm)[a]	−372 (348 nm)	−578 (230 nm)	−0.014 (379 nm)	0.09%	0.002

[a] Values are reprinted from literature.[8]

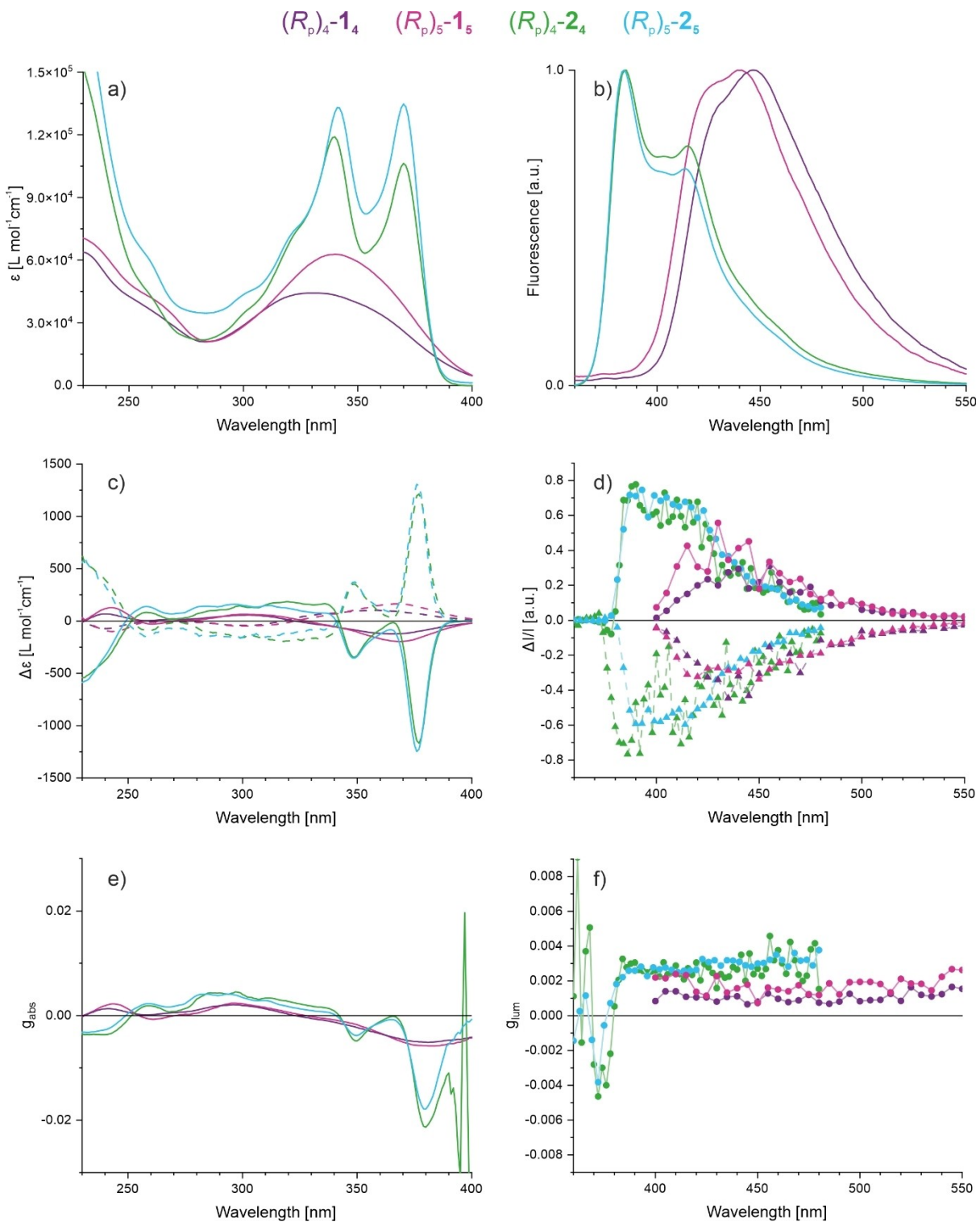

Figure 4. Optical and chiroptical properties of the tetrameric and pentameric structures of both libraries $(R_p)_n$-**1**$_n$ and $(R_p)_n$-**2**$_n$ in CH_2Cl_2. The spectra for trimeric and hexameric structures were omitted for clarity but can be found in the Supporting Information. a. Absorption. b. Emission. c. CD of the *R* enantiomer (solid line) and the *S* enantiomer (dashed line). d. Scaled intensity difference of the CPL of the *R* enantiomer (solid line) and the *S* enantiomer (dashed line) multiplied by a factor of 500. The collected datapoints are reported with symbols and joined with a line. e. g_{abs} of the *R* enantiomer. f. g_{lum} of the *R* enantiomer.

and are reported in Figure 4c. A constant g_{lum} value of 0.003 with an unexpected sign inversion at 370 nm was observed for both enantiomers of the $(R_p)_n$-**2**$_n$ library. Such changes have been observed for other paracyclophanes,[24] polyfuranes,[25] and other compounds.[26] The overlap of this sign change with the absorption spectrum could also be an indication that reflected,

emitted light is autoabsorbed. The discussed bathochromic shift observed for the emission maxima of the thiophene derivatives was confirmed in the CPL measurements. As expected from the CD spectra, a significant decrease in $\Delta I/I$ was observed for the $(R_p)_n$-**1**$_n$ library compared to the $(R_p)_n$-**2**$_n$ one. The trend in CPL intensity observed for the different cyclophane sizes within a library was comparable, resulting in the emission of circularly polarized light accounting for 0.04% and 0.08% of the light emission for $(R_p)_4$-**1**$_4$ and $(R_p)_5$-**1**$_5$ respectively. The calculated g_{lum} values remain constant at 0.002 across the wavelength of the luminescence spectrum. Notably, as reported for the absorption, no vibrational substructure was present in thiophene derivatives and the inversion of sign for g_{lum} values was not observed either. The measured g_{lum} values are similar to previously reported *para*-cyclophane derivatives and no amplification was observed by the circular arrangement of the subunits.[27,28]

Computational analysis

Time-dependent density-functional theory (TDDFT) calculations were performed on $(S_p)_n$-**1**$_n$ and $(S_p)_n$-**2**$_n$ enantiomers. The structures were geometry optimized from the crystal structure as starting point using a B3PW91 functional with a 6-31G(d,p) basis set.[29,30] Molecular orbital depictions of the HOMO and LUMO are presented in Figure 5. Highly symmetric electronic and nuclear structures were observed for $(S_p)_4$-**2**$_4$ and $(S_p)_5$-**2**$_5$, whereas $(S_p)_4$-**1**$_4$ and $(S_p)_5$-**1**$_5$ show little symmetry. The lack of symmetry in these thiophene structures are caused by significant steric crowding that is absent in the 1,3-butadiyne connections. This lack of symmetry causes the cyclophane units to experience non-identical electronic environments in the crowded thiophene-linked ring systems. These slight environmental differences even out the vibrational features in the luminescence spectrum that can be regarded as a composite of the individual chromophoric unit's light emission.

The theoretical UV absorption and CD transitions were also calculated and modeled with the following relationships:

$$\varepsilon = \frac{2.175 \times 10^8}{\sigma} \sum_i f_i \; exp\left[-\left(\frac{v - v_i}{\sigma}\right)^2\right]$$

$$\Delta\varepsilon = \frac{1}{2.296 \times 10^{-39}} \frac{1}{\sigma\sqrt{\pi}} \sum_i v_i \; R_i \; exp\left[-\left(\frac{v - v_i}{\sigma}\right)^2\right]$$

Where f_i, v_i and R_i are the oscillator strengths, energies and rotary strengths of each transition. σ was set to 0.4 eV to simulate the broadening of the electronic transitions by vibrations and rotations. The Python code for modeling CD and UV-Vis spectra is included in the Supporting Information.

The 1,3-butadiyne derivatives, $(S_p)_n$-**2**$_n$, show a bathochromic shift of 30 nm in the calculated UV absorption maxima when compared to the experimentally observed results (see Figure S23 in the Supporting Information). A similar shift is also seen for the simulated CD spectral maxima. Difficulties in calculating butadiyne-containing compounds have been reported in our prior work.[31] Nonetheless, the three Cotton bands as seen in Figure 4 were replicated by the DFT calculations with the correct signs, but exhibit a blue shift that is not unusual for such calculations, especially for transitions in the blue/UV region (see Figure S23).[32] The modelling for the electronic absorption and the CD is more accurate for the $(S_p)_n$-**1**$_n$ library (see Figure S23 in the Supporting Information). The calculated CD spectra of the thiophene derivatives were weaker compared to the 1,3-butadiyne ones and showed the three cotton bands, with the initial band again predicting the sign of the *Cotton* effect accurately for the selected chirality of the

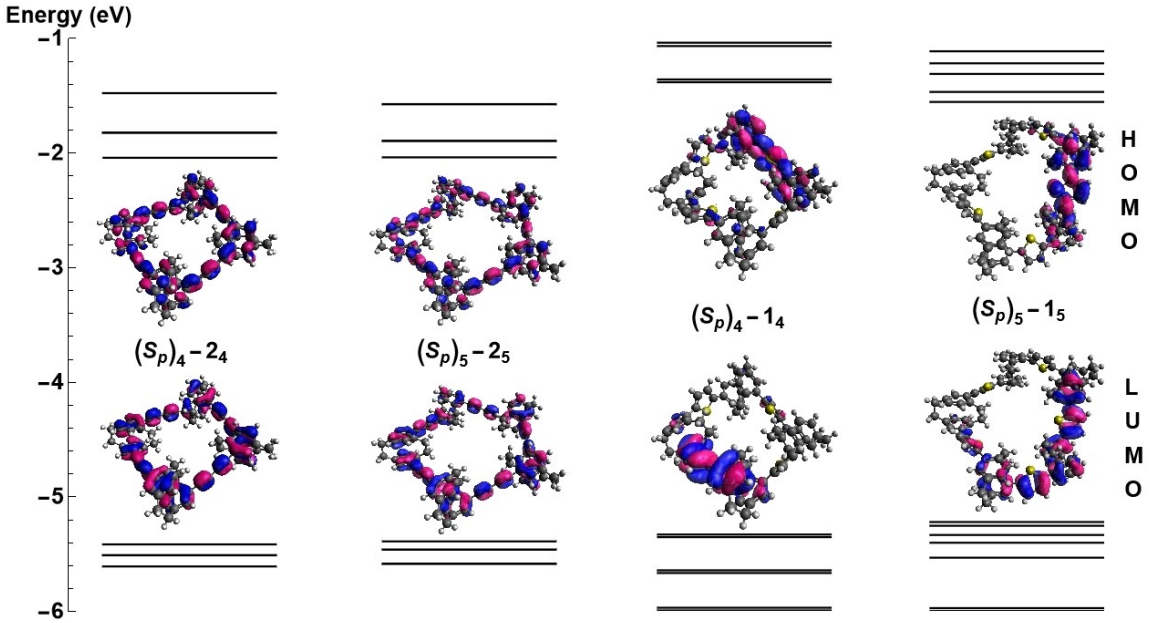

Figure 5. Calculated orbital energies and frontier orbital structures corresponding to $(S_p)_n$-**1**$_n$ and $(S_p)_n$-**2**$_n$.

input geometry, but the measured spectrum lacked the bisignate circular dichroism effect present in the calculated spectrum at 320 nm. The calculations correctly predict that the measured signal is weaker than that of the parent 1,3-butadiyne species, but underestimates the magnitude of the decrease.

Conclusions

The herein reported enantiopure heterocyclized tetrameric and pentameric macrocycles $(R_p)_4$-**1**$_4$/$(S_p)_4$-**1**$_4$ and $(R_p)_5$-**1**$_5$/$(S_p)_5$-**1**$_5$ were synthesized in a single step from the previously reported polygon-shaped structures. We could show that transforming a 1,3butadiyne unit to a 2,5thienyl leads to a desired increase of the quantum yield and a significant redshift in emission wavelengths, presumably due to the donating effect of the electron-rich thiophene moiety. Solid-state structure analysis revealed a high flexibility of the thiophene units, also contributing to the much larger *Stokes* shift as compared to the 1,3 butadiyne-linked macrocycles. Concurrently, the CD and CPL activity, which heavily depend on the molecular geometry, dropped approximately by a factor of two and three for the different ring sizes of the thienyl-linked structures. Notwithstanding, the absorption and luminescence dissymmetry factors g_{abs} and g_{lum} are in the range of 10^{-3} and thus remain in the region of average chiral small molecule fluorophores. Unexpectedly, the CPL experiment of the 1,3-butadiyne linked library $(R_p)_n$-**2**$_n$ revealed moderate g_{lum} values of 0.003, despite displaying large g_{abs} values. The suggested correlation of $|g_{lum}| = 0.94 \times |g_{abs}|$ is thus not applicable for this library of compounds and we hope to shine light on this matter by investigating the excited state structure and orientation of transition dipole moments. Also, we aim at reducing the flexibility of the thiophene units by covalently linking it to the PCP phenylenes and introducing an electron-withdrawing unit to retain the intense chiroptics along with the redshifted absorption. We are optimistic that the sophisticated optimization of the structure of pseudo-*meta* PCP macrocycles will make exceptional CPL emitters accessible.

Supporting Information

In the Supporting Information, we cite the work by Oyler *et al.* describing the setup used to record the CPL spectra.[33] In the description of the crystal structure in the Supporting Information we furthermore reference to the work of Dolomanov *et al.*[34] and of Sheldrick.[35,36]

Deposition Number 2293691 ($(S_p)_4$-**1**$_4$) contains the supplementary crystallographic data for this paper. These data are provided free of charge by the joint Cambridge Crystallographic Data Centre and Fachinformationszentrum Karlsruhe Access Structures service.

Acknowledgements

The Bernhard group gratefully acknowledges support by the US NSF under grant CHE-2102460. P. D. was partially supported through a Beckman Foundation Undergraduate Research Fellowship. The Mayor group acknowledges generous support by the Swiss National Science Foundation (200020_207744). Open Access funding provided by Universität Basel.

Conflict of Interests

The authors declare no conflict of interest.

Data Availability Statement

The data that support the findings of this study are available in the supplementary material of this article.

Keywords: circularly polarized luminescence · heterocyclization · macrocycle · molar circular dichroism · [2.2]paracyclophane · 2,5-thienyl

[1] C. J. Brown, A. C. Farthing, *Nature* **1949**, *164*, 915.
[2] K. J. Weiland, A. Gallego, M. Mayor, *Eur. J. Org. Chem.* **2019**, *2019*, 3073.
[3] D. J. cram, J. M. Cram, *Acc. Chem. Res.* **1971**, *4*, 204.
[4] K. Reznikova, C. Hsu, W. M. Schosser, A. Gallego, K. Beltako, F. Pauly, H. S. J. van der Zant, M. Mayor, *J. Am. Chem. Soc.* **2021**, *143*, 13944.
[5] H. J. Reich, D. J. Cram, *J. Am. Chem. Soc.* **1969**, *91*, 3517.
[6] M. Hasegawa, Y. Ishida, H. Sasaki, S. Ishioka, K. Usui, N. Hara, M. Kitahara, Y. Imai, Y. Mazaki, *Chem. Eur. J.* **2021**, *27*, 16225.
[7] Y. Morisaki, K. Inoshita, Y. Chujo, *Chem. Eur. J.* **2014**, *20*, 8386.
[8] E. Sidler, P. Zwick, C. Kress, K. Reznikova, O. Fuhr, D. Fenske, M. Mayor, *Chem. Eur. J.* **2022**, *28*, e202201764.
[9] J. He, M. Yu, M. Pang, Y. Fan, Z. Lian, Y. Wang, W. Wang, Y. Liu, H. Jiang, *Chem. Eur. J.* **2022**, *28*, e202103832.
[10] Y. Wu, G. Zhuang, S. Cui, Y. Zhou, J. Wang, Q. Huang, P. Du, *Chem. Commun.* **2019**, *55*, 14617.
[11] X. Li, A. Staykov, K. Yoshizawa, *Bull. Chem. Soc. Jpn.* **2012**, *85*, 181.
[12] H. Tanaka, Y. Inoue, T. Mori, *ChemPhotoChem* **2018**, *2*, 386.
[13] Y. Deng, M. Wang, Y. Zhuang, S. Liu, W. Huang, Q. Zhao, *Light-Sci. Appl.* **2021**, *10*, 76.
[14] A. D'Addio, J. Malinčik, O. Fuhr, D. Fenske, D. Häussinger, M. Mayor, *Chem. Eur. J.* **2022**, *28*, e202201678.
[15] C. Schaack, L. Arrico, E. Sidler, M. Górecki, L. Di Bari, F. Diederich, *Chem. Eur. J.* **2019**, *25*, 8003.
[16] C. Schaack, E. Sidler, N. Trapp, F. Diederich, *Chem. Eur. J.* **2017**, *23*, 14153.
[17] Q. Zheng, R. Hua, J. Jiang, L. Zhang, *Tetrahedron* **2014**, *70*, 8252.
[18] G. Zhang, H. Yi, H. Chen, C. Bian, C. Liu, A. Lei, *Org. Lett.* **2014**, *16*, 6156.
[19] Y. Yang, M. Chu, Q. Miao, *Org. Lett.* **2018**, *20*, 4259.
[20] B. V. Phulwale, S. K. Mishra, M. Nečas, C. Mazal, *J. Org. Chem.* **2016**, *81*, 6244.
[21] G. Snatzke, *Angew. Chem.* **1979**, *91*, 380.
[22] N. Berova, L. D. Bari, G. Pescitelli, *Chem. Soc. Rev.* **2007**, *36*, 914.
[23] J. Roose, S. Achermann, O. Dumele, F. Diederich, *Eur. J. Org. Chem.* **2013**, *2013*, 3223.
[24] Z. Lian, L. Liu, J. He, S. Fan, S. Guo, X. Li, G. Liu, Y. Fan, X. Chen, M. Li, C. Chen, H. Jiang, *Chem. - Eur. J. n/a*, e202303819.
[25] M. Kawakami, P. Downey, L. Peteanu, S. Bernhard, K. J. T. Noonan, *Polym. J.* **2023**, *55*, 565.
[26] S. Thi Duong, M. Fujiki, *Polym. Chem.* **2017**, *8*, 4673.
[27] S. Ishioka, M. Hasegawa, N. Hara, H. Sasaki, Y. Nojima, Y. Imai, Y. Mazaki, *Chem. Lett.* **2019**, *48*, 640.
[28] M. Gon, Y. Morisaki, Y. Chujo, *J. Mater. Chem. C* **2014**, *3*, 521.

[29] A. D. Becke, *J. Chem. Phys.* **1993**, *98*, 5648.
[30] M. J. Frisch, G. W. Trucks, H. B. Schlegel, G. E. Scuseria, M. A. Robb, J. R. Cheeseman, G. Scalmani, V. Barone, G. A. Petersson, H. Nakatsuji, X. Li, M. Caricato, A. V. Marenich, J. Bloino, B. G. Janesko, R. Gomperts, B. Mennucci, H. P. Hratchian, J. V. Ortiz, A. F. Izmaylov, J. L. Sonnenberg, D. Williams-Young, F. Ding, F. Lipparini, F. Egidi, J. Goings, B. Peng, A. Petrone, T. Henderson, D. Ranasinghe, V. G. Zakrzewski, N. Gao, N. Rega, G. Zheng, M. Liang, M. Hada, M. Ehara, K. Toyota, R. Fukuda, J. Hasegawa, M. Ishida, T. Nakajima, Y. Honda, O. Kitao, H. Nakai, T. Vreven, K. Throssell, J. A. Montgomery, J. E. Peralta, F. Ogliaro, M. J. Bearpark, J. J. Heyd, E. N. Brothers, K. N. Kudin, V. N. Staroverov, T. A. Keith, R. Kobayashi, J. Normand, K. Raghavachari, A. P. Rendell, J. C. Burant, S. S. Iyengar, J. Tomasi, M. Cossi, J. M. Millam, M. Klene, C. Adamo, R. Cammi, J. W. Ochterski, R. L. Martin, K. Morokuma, O. Farkas, J. B. Foresman, D. J. Fox, *Gaussian 16, Revision C.01*, **2016**.
[31] T. Brandl, V. Hoffmann, A. Pannwitz, D. Häussinger, M. Neuburger, O. Fuhr, S. Bernhard, O. S. Wenger, M. Mayor, *Chem. Sci.* **2018**, *9*, 3837.
[32] F. J. Coughlin, K. D. Oyler, R. A. Pascal, S. Bernhard, *Inorg. Chem.* **2008**, *47*, 974.
[33] K. D. Oyler, F. J. Coughlin, S. Bernhard, *J. Am. Chem. Soc.* **2007**, *129*, 210.
[34] O. V. Dolomanov, L. J. Bourhis, R. J. Gildea, J. a. K. Howard, H. Puschmann, *J. Appl. Crystallogr.* **2009**, *42*, 339.
[35] G. M. Sheldrick, *Acta Crystallogr. Sect. A* **2015**, *71*, 3.
[36] G. M. Sheldrick, *Acta Crystallogr. Sect. C* **2015**, *71*, 3.

Manuscript received: December 5, 2023
Accepted manuscript online: January 12, 2024
Version of record online: January 30, 2024